Available online at www.sciencedirect.com

ScienceDirect

Nuclear Physics B 903 (2016) 360–373

NUCLEAR PHYSICS B

www.elsevier.com/locate/nuclphysb

Holographic vector superconductor in Gauss–Bonnet gravity

Jun-Wang Lu [a,*], Ya-Bo Wu [b], Tuo Cai [a], Hai-Min Liu [a], Yin-Shuan Ren [a], Mo-Lin Liu [c]

[a] *Department of Physics and Electronic Science, Qiannan Normal College for Nationalities, Duyun 558000, PR China*
[b] *Department of Physics, Liaoning Normal University, Dalian 116029, PR China*
[c] *College of Physics and Electronic Engineering, Xinyang Normal University, Xinyang 464000, PR China*

Received 27 December 2015; accepted 4 January 2016

Available online 7 January 2016

Editor: Stephan Stieberger

Abstract

In the probe limit, we numerically study the holographic p-wave superconductor phase transitions in the higher curvature theory. Concretely, we study the influences of Gauss–Bonnet parameter α on the Maxwell complex vector model (MCV) in the five-dimensional Gauss–Bonnet–AdS black hole and soliton backgrounds, respectively. In the two backgrounds, the improving Gauss–Bonnet parameter α and dimension of the vector operator Δ inhibit the vector condensate. In the black hole, the condensate quickly saturates a stable value at lower temperature. Moreover, both the stable value of condensate and the ratio ω_g/T_c increase with α. In the soliton, the location of the second pole of the imaginary part increases with α, which implies that the energy of the quasiparticle excitation increases with the improving higher curvature correction. In addition, the influences of the Gauss–Bonnet correction on the MCV model are similar to the ones on the SU(2) p-wave model, which confirms that the MCV model is a generalization of the SU(2) Yang–Mills model even without the applied magnetic field to some extent.

* Corresponding author.
E-mail address: lujunwang.2008@163.com (J.-W. Lu).

http://dx.doi.org/10.1016/j.nuclphysb.2016.01.010

1. Introduction

The gauge/gravity duality [1,2] shows that a $(d+1)$-dimensional weak gravity system corresponds to a d-dimensional strongly coupled conformal field theory on its boundary, which thus provides us a feasible and efficient approach for studying the system involving the strong interaction, especially the high temperature superconductors.

In Ref. [3], the first holographic s-wave superconductor model was numerically realized in the four-dimensional Schwarzschild anti-de Sitter (AdS) black hole coupled to the Maxwell complex scalar field. The results showed that below a critical temperature, the scalar "hair" appears outside the horizon, which spontaneously breaks the U(1) gauge symmetry of the system. This corresponds to the spontaneous breaking of the global U(1) symmetry from the holographic dictionary, and thus models the s-wave superconductor phase transition. Thereafter, Refs. [4,5] constructed holographic p-wave and d-wave superconductors, respectively. Except the numerical approach, that the Sturm–Liouville (SL) eigenvalue approach [6] as well as the matching method [7] are showed to be efficient for the critical behavior of the superconductor phase transition. It should be noted that all above works based on the probe limit, away from which the holographic model was further investigated in Ref. [8]. Considering that there exists a mass gap in the insulator, the authors of Ref. [9] modeled the insulator/superconductor phase transition in the five-dimensional AdS soliton. Moreover, the holographic superconductor models were studied in the system involving the magnetic field [10,11]. Because the Mermin–Wagner (or Coleman) theorem forbids continuous symmetry to be spontaneously broken in three-dimensional spacetimes at finite temperature, the study of the higher curvature theory to construct holographic superconductors attracted a lot of attention, especially the five-dimensional Gauss–Bonnet gravity with high curvature correction, see, for example, [12–28], where the results showed that the increasing Gauss–Bonnet correction inhibits the phase transition.

On the other hand, similar to the construction of the s-wave superconductor [3,29–31], a holographic p-wave superconductor model was proposed in the four-dimensional Schwarzschild AdS black hole coupled to a Maxwell complex vector (MCV) field in the probe limit [32]. It was showed that, for the lowest Landau level, the applied magnetic field can induce the vector condensate, which is reminiscent of the QCD vacuum phase transition [33–35], while for the excited Landau level, the magnetic field effect on the MCV superconductor is similar to the ordinary superconductors [10,11]. In Ref. [36], the holographic insulator/superconductor phase transition induced by the magnetic field was studied in the five-dimensional AdS soliton coupled to such a MCV field and the SU(2) Yang–Mills (YM) field, respectively. It was shown that the MCV model is a generalization of the SU(2) model with general mass, charge. Subsequently, Refs. [37,38] studied respectively the Lifshitz and Gauss–Bonnet effects on the MCV superconductor model induced by the magnetic field, and found that the increasing Gauss–Bonnet parameter always hinders the vector condensate. Considering the backreaction of the MCV field on the AdS gravity spacetime, Refs. [39–43] further studied the holographic vector condensate and its related complete phase diagrams as well as entanglement entropy, and obtained the rich phase structures, especially the "retrograde condensate". Then, the coexistence and competition of ferromagnetism and MCV superconductivity were studied in Ref. [44], which showed that the results depend partly on the self-interaction of magnetic moment of the complex vector field. The authors of Ref. [45] investigated the MCV model in the four-dimensional Einstein–Born–Infeld AdS theory away from the probe limit, and obtained the rich and varied phase structure depending on the mass parameter m, the backreaction parameter κ as well as the Born–Infeld parameter γ. In the probe limit, the authors of Ref. [46] numerically and analytically studied the effect of the

Weyl corrections on the MCV superconductor in the AdS soliton and black hole, and found that the larger Weyl correction enhances the conductor/superconductor phase transition but has no effects on the insulator/superconductor transition. In Ref. [47], the effect of dark mater on the MCV model was analytically studied in the probe limit and thus found to be same with the case of the s-wave model. As for this MCV model, in Refs. [48,49], we realized the p-wave superfluid in the AdS and Lifshitz black holes, respectively. Thus we respectively studied the effects of the Lifshitz and Gauss–Bonnet parameters on the superconductor phase transition induced by the magnetic field [37,38]. In particular, we built the conductor/superconductor and insulator/superconductor phase transition triggered by the applied magnetic field in the Gauss–Bonnet AdS black hole and soliton spacetimes, and found that the increasing Gauss–Bonnet parameter always hinders the vector condensate in two backgrounds. However, in the previous work [38], we mainly payed our attention on the influence of the magnetic field inducing the vector condensate and only considered the effect of the Gauss–Bonnet parameter on the critical behaviors but not calculated the one on the condensate as well as the frequency dependent conductivity. To make up this gap, it is interesting to explore the effects of the higher curvature theory on the vector condensate as well as the conductivity in the conductor/superconductor and insulator/superconductor models, for example, the Gauss–Bonnet gravity, which is our motivation in this paper.

Based on the above motivation, we will respectively construct the holographic p-wave superconductor phase transition by coupling the MCV field to the Gauss–Bonnet–AdS black hole and soliton backgrounds at the probe approximation. For both the black hole and soliton backgrounds, it is observed that the increasing Gauss–Bonnet correction makes the phase transition become more difficult. Moreover, near the critical value, the vector condensates have a square root behavior as expected from the mean field theory. In addition, the ratio of the energy gap and the critical value in the conductor/superconductor much larger than the BCS value indicates that the holographic model indeed includes the strong interaction.

The organization of this paper is as follows. In Sec. 2, in the probe limit, we numerically study the holographic p-wave conductor/superconductor phase transition in the five-dimensional Gauss–Bonnet–AdS black hole background coupled to the MCV field, and thus calculate the conductivity as a function of the frequency. Similar to the process in Sec. 2, the insulator/superconductor phase transition is studied in Gauss–Bonnet–AdS soliton background in Sec. 3. The final section is devoted to conclusions and discussions.

2. Conductor/superconductor phase transition

In this section, we study the vector condensate in the Gauss–Bonnet–AdS black hole coupled to the MCV field, which is followed by the frequency depended conductivity.

The five-dimensional Ricci flat Gauss–Bonnet–AdS black hole is of the form [12]

$$\begin{aligned} ds^2 &= -r^2 f(r)dt^2 + \frac{dr^2}{r^2 f(r)} + r^2(dx^2+dy^2+dz^2), \\ f(r) &= \frac{1}{2\alpha}\left(1-\sqrt{1-\frac{4\alpha}{L^2}(1-\frac{ML^2}{r^4})}\right), \end{aligned} \tag{1}$$

where M and L denote the mass of the black hole and the AdS radius, respectively, while the constant α represents the Gauss–Bonnet coupling with the upper bound, i.e., the so-called Chern–Simons limit $\alpha = L^2/4$. Considering further the constraints of the causality via the holographic

correspondence [50], the Gauss–Bonnet parameter has the range $-7L^2/36 \leq \alpha \leq 9L^2/100$, which we will take in the present paper. Meanwhile, the Hawking temperature of the black hole reads $T = \frac{r_+}{\pi L^2}$, where $r_+ = \sqrt[4]{ML^2}$ represents the location of the horizon, which satisfies $f(r_+) = 0$. Near the asymptotical infinity, the metric function is given by

$$f(r) \sim \frac{1}{2\alpha}\left(1 - \sqrt{1 - \frac{4\alpha}{L^2}}\right). \tag{2}$$

Thus, we can define an effective AdS radius L_{eff} as [14]

$$L_{eff}^2 = \frac{2\alpha}{1 - \sqrt{1 - \frac{4\alpha}{L^2}}}. \tag{3}$$

Following Ref. [32], we consider the matter action including a Maxwell field and a complex vector field

$$\begin{aligned}\mathcal{S}_{MCV} = \frac{1}{16\pi G_5}\int dx^5\sqrt{-g}\Big(&-\frac{1}{4}F_{\mu\nu}F^{\mu\nu} - \frac{1}{2}(D_\mu\rho_\nu - D_\nu\rho_\mu)^\dagger(D^\mu\rho^\nu - D^\nu\rho^\mu)\\ &- m^2\rho_\mu^\dagger\rho^\mu + iq\gamma\rho_\mu\rho_\nu^\dagger F^{\mu\nu}\Big),\end{aligned} \tag{4}$$

where $F_{\mu\nu} = \nabla_\mu A_\nu - \nabla_\nu A_\mu$ is the strength of the U(1) gauge field A_μ, and $D_\mu = \nabla_\mu - iqA_\mu$, while m and q correspond to the mass and the charge of the vector field ρ_μ. We do not consider the magnetic field effects on the superconductor transition, so the last term with the constant γ is ignored, which characterizes the strength of interaction between ρ_μ and $F_{\mu\nu}$.

From the action (4), equations of motion of ρ_μ and A_μ are given by

$$D^\nu(D_\nu\rho_\mu - D_\mu\rho_\nu) - m^2\rho_\mu = 0, \tag{5}$$

$$\nabla^\nu F_{\nu\mu} - iq(\rho^\nu(D_\nu\rho_\mu - D_\mu\rho_\nu)^\dagger - \rho^{\nu\dagger}(D_\nu\rho_\mu - D_\mu\rho_\nu)) = 0. \tag{6}$$

Comparing with the Gauss–Bonnet–AdS gravity, we regard the matter sector (4) as a probe realized by taking $q \to \infty$ with $q\rho_\mu$ and $qA\mu$ fixed. At this approximation, Eqs. (5) and (6) decouple from the equations of gravitational sector.

To construct the p-wave superconductor induced by the gauge field, we take the ansatz for the vector field ρ_μ and the gauge field A_μ as the following form

$$\rho_\nu dx^\nu = \rho_x(r)dx,\ A_\nu dx^\nu = \phi(r)dt, \tag{7}$$

with other components vanishing. Choosing $\rho_x(r)$ and $\phi(r)$ as real functions and substituting the above ansatz (7) into Eq. (5), we can read off the equations for ρ_x and ϕ

$$\psi''(r) + \left(\frac{f'(r)}{f(r)} + \frac{3}{r}\right)\psi'(r) + \left(\frac{\phi(r)^2}{r^4 f(r)^2} - \frac{m^2}{r^2 f(r)}\right)\psi(r) = 0, \tag{8}$$

$$\phi''(r) + \frac{3}{r}\phi'(r) - \frac{2\psi(r)^2}{r^4 f(r)}\phi(r) = 0, \tag{9}$$

where the prime denotes the derivative with respect to r. Comparing Eqs. (8) and (9) with Eqs. (7) in Ref. [15], it is observed that the equations are similar to each other except the additional factor "2" of ϕ in Eq. (9), from which we can expect that the features of the MCV model resemble the ones of the SU(2) Yang–Mills model. To solve the above equations, we should impose the boundary conditions. At the horizon, the vector field ρ_μ is required to be regular, while the gauge

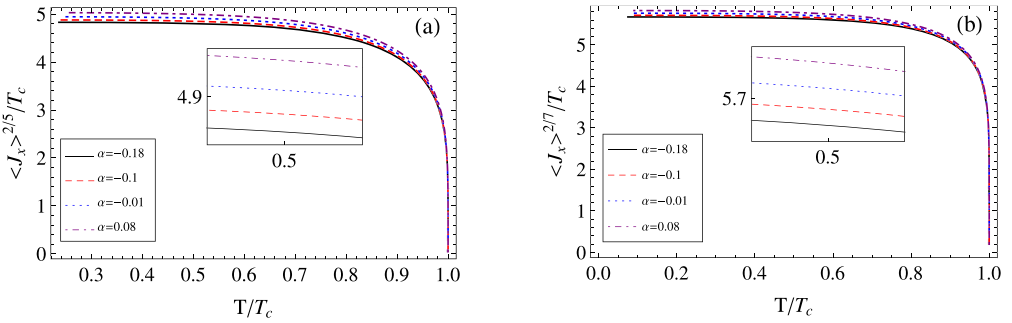

Fig. 1. The condensation versus temperature for $\Delta = 3/2$ (left) and $\Delta = 5/2$ (right). The curves in both two subfigures from top to bottom correspond to $\alpha = -0.18$ (solid), -0.1 (dashed), -0.01 (dotted), 0.08 (dotdashed), respectively.

field A_μ should satisfy the condition $\phi(r_+) = 0$ to ensure the finite form of $g^{\mu\nu}A_\mu A_\nu$. Near the infinite boundary, the general expansions of the matter field and the gauge field are given by

$$\psi(r) = \frac{\psi_-}{r^{\Delta_-}} + \frac{\psi_+}{r^{\Delta_+}} + \ldots, \tag{10}$$

$$\phi(r) = \mu - \frac{\rho}{r^2} + \ldots, \tag{11}$$

where $\Delta_\pm = 1 + \sqrt{L_{eff}^2 m^2 + 1}$ with the Breitenlohner–Freedman (BF) bound of the mass $m^2 \geq m_{BF}^2 = -1/L_{eff}^2$. According to the gauge/gravity duality, the coefficients of the leading term ψ_- and the subleading term ψ_+ are interpreted as the source and the vacuum-expectation value of the boundary operator J_x, while μ and ρ are regarded as the chemical potential and the charge density in the dual field theory, respectively. To guarantee the U(1) gauge symmetry of the system breaking spontaneously, we require that the source of the condensate vanishes, i.e., $\psi_- = 0$.

There is an important symmetry in the above system with the form

$$(r, T) \to \lambda(r, T), \psi_+ \to \lambda^{\Delta+1}\psi_+, \rho \to \lambda^3\rho \tag{12}$$

with the positive constant λ. By using Eq. (12) we can fix the charge density ρ of the system and thus work in the canonical ensemble.

Next, we solve the above nonlinear ordinary differential equations by the familiar shooting method. In this work we focus on the effects of the high curvature corrections (i.e., the parameter α) on the critical temperature and the vector condensate as well as the conductivity, so we will fix the dimension of the boundary operator Δ_+, which is regarded as the "mass" in the dual field. As a special case, we take $\Delta_+ = \Delta = 3/2, 5/2$ in the following calculations, respectively. We plot the condensate as a function of the temperature for $\Delta_+ = 3/2$ and $\Delta_+ = 5/2$ in Fig. 1, and also list the critical temperature as well as the condensate by fitting the numerical curves in Table 1, from which we get the following results. Firstly, for all cases, there is a critical temperature, below which the vector field begins to condense. Moreover, the critical temperature decreases with the increasing Gauss–Bonnet parameter, which indicates that the increasing high curvature correction hinders the conductor/superconductor phase transition. To compare the results with the ones in Ref. [38], we additionally calculate the critical temperature for different values of α with $\Delta = 3/2$. The concrete results are $T_c = 0.2350\rho^{1/3}(\alpha = -19/100)$, $T_c = 0.2275\rho^{1/3}(\alpha = -5/100)$ and $T_c = 0.2172\rho^{1/3}(\alpha = 9/100)$, which agrees with the results in Figs. (3) and (4) in Ref. [38]. Secondly, near the critical point, the square root dependence

Table 1
The critical temperature and condensate as a function of the Gauss–Bonnet parameter α, where the vacuum-expectation value $\langle J_x \rangle$ is calculated near the critical temperature T_c.

α	-0.18	-0.1	-0.01	0.08
$T_c/\rho^{1/3}(\Delta = 3/2)$	0.2346	0.2304	0.2250	0.2182
$\langle J_x \rangle / T_c^{5/2}(\Delta = 3/2)$	114.0	117.0	120.0	124.9
$T_c/\rho^{1/3}(\Delta = 5/2)$	0.1923	0.1889	0.1845	0.1790
$\langle J_x \rangle / T_c^{7/2}(\Delta = 5/2)$	990.0	1000.0	1030.0	1050.0

of the vector condensate on the temperature indicates that the critical exponent $1/2$ is universal for all cases, and thus suggests that the system undergoes a second-order transition as expected from the mean field theory. What is more, the fitting coefficients near the critical temperature increases with the parameter α, which is consistent with the fact that the larger α makes the phase transition more difficult. Thirdly, when the temperature decreases gradually, the condensate for all cases tends to be a stable constant increasing with α, which agrees with the above result (i.e., the larger α hinders the transition). The effect of α on the condensate is similar to the one on the condensate of the SU(2) p-wave [15] as well as the s-wave [19] condensates. Meanwhile, the stable constant of the condensate is larger than the weak coupling BCS theory value 3.5, which indicates that the present p-wave model indeed describes a strongly coupled field theory. Lastly, comparing the critical value in the different case of the dimension (Δ) of the operator with each other for the fixed parameter α in Table 1, the critical value always decreases when Δ increases from $3/2$ to $5/2$, which is reasonable, if we consider the dimension Δ as the "mass" in the dual field theory.

As we all know, the infinite DC conductivity is the typical signal to distinguish the state is either in superconducting sate or not. Meanwhile, we can read off the energy gap from the frequency dependent conductivity and thus explore the strength of the interaction in the system, so it is helpful for us to study the conductivity. To obtain the conductivity, which is related to the retarded Green function, $\sigma(\omega) = G^R(\omega, k = 0)/i\omega$, we can calculate the perturbation of the gauge field based on the superconducting state in the gravitation spacetime from the holographic dual dictionary [2,3,30]. It should be noted that below the critical temperature, the condensate of the vector operator J_x breaks the U(1) gauge symmetry as well as the rotational symmetry, therefore, it is natural that the conductivity along the condensing direction is different from that perpendicular to the condensing direction. From the calculation for the conductivity along the condensing direction in Ref. [4], one can imagine the perturbation of the complex vector field ρ_μ along the x direction is rather complicated. For simplicity, following Refs. [32,42,45], we focus on our calculations perpendicular to the superconducting direction with the ansatz $\Delta A_\mu = A_y(r)e^{-i\omega t}$. Substituting the ansatz into Eq. (6), the linearized equation of the perturbation A_y is of the form

$$A_y''(r) + \left(\frac{f'(r)}{f(r)} + \frac{3}{r}\right) A_y'(r) + \left(\frac{\omega^2}{r^4 f(r)^2} - \frac{2\psi(r)^2}{r^4 f(r)}\right) A_y(r) = 0, \tag{13}$$

which is the same as Eq. (20) in Ref. [15] and also similar to the corresponding equations in Refs. [3,4]. At the horizon, the retarded Green function G^R corresponds to the ingoing wave condition, therefore, $A_y(r)$ can be expressed as

$$A_y(r) = (r - r_+)^{-i\omega/\pi T} \left(1 + A_{y1}(r - r_+) + A_{y2}(r - r_+)^2 + A_{y3}(r - r_+)^3 + \cdots\right). \tag{14}$$

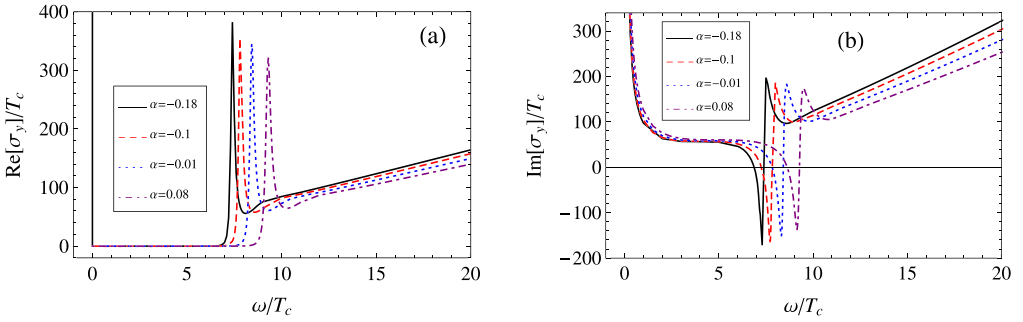

Fig. 2. The real (a) and imaginal (b) part of the AC conductivity versus the frequency near $T/T_c \approx 0.3$ in the case of $\Delta = 3/2$. The curves in both two subfigures from top to bottom correspond to $\alpha = -0.18$ (solid), -0.1 (dashed), -0.01 (dotted), 0.08 (dotdashed), respectively.

At the boundary $r \to \infty$, the general falloff of $A_x(r)$ reads

$$A_x(r) = A^{(0)} + \frac{A^{(2)}}{r^2} + \frac{A^{(0)}\omega^2 L_{eff}^4}{2}\frac{log\Lambda r}{r^2} + \cdots . \tag{15}$$

According to the gauge/gravity duality, the Green function G^R can be calculated from the gauge field perturbation, which has the form

$$G^R = -\lim_{r\to\infty} r^3 f \frac{A_y'(r)}{A_y(r)}. \tag{16}$$

There is a logarithmic divergence term in the Green function as well as the conductivity, which has been canceled by the holographic renormalization. The final conductivity can be expressed as

$$\sigma(\omega) = \frac{G^R}{i\omega} = \frac{-2iA^{(2)}}{\omega L_{eff}^2 A^{(0)}} + \frac{i\omega L_{eff}^2}{2}, \tag{17}$$

which is same with Eq. (20) in Ref. [15]. The conductivity as a function of the frequency for different value of the parameter α in the case of $\Delta = 3/2$ is plotted in Fig. 2, from which we can obtain the following results. Firstly, at the zero frequency, there exists a pole in the imaginary part of the conductivity, which is the signal of the infinite DC conductivity in the superconducting state from the Kramers–Kronig (KK) relation. Secondly, as we know, in Ref. [29], the second even more pole appears in the case of $m^2 = m_{BF}^2$ when the temperature is obviously lower than the critical value. Here we find that there is still a second pole when $m^2 > m_{BF}^2$ when $T/T_c \approx 0.3$, which corresponds to a spike in the real part of the conductivity. This spike also appears in Refs. [16,30,51]. From the gravity standpoint [15,29], the spikes are contributed to the fact that the quasinormal mode becomes an actual model in the present case. Thirdly, if we define the ratio of the energy gap and the critical temperature (ω_g/T_c) as the minimum of the imaginary part of the conductivity when $m^2 > m_{BF}^2$ [29], the location of the second pole in the conductivity stands for ω_g/T_c. From Fig. 2(b), for the fixed temperature, the ratio ω_g/T_c is always much larger than 3.5, which indicates that the holographic superconductor models the strong interaction. Meanwhile, the energy gap increases with the Gauss–Bonnet parameter α, which implies the larger α hinders the superconductor phase transition. Fourthly, when the frequency tends to

be infinity, both the real and imaginal parts of the conductivity diverge, which might be the general property in the five-dimensional AdS black holes, except for the Lifshitz gravity with the dynamical critical exponent $z > 1$ [52]. In addition, we also study the effects of the dimension of the vector operator Δ on the frequency dependent conductivity. In particular, we calculate the conductivity for different value of α when $\Delta = 5/2$ and $T/T_c \approx 0.3$. It is observed that there is always a pole corresponding to superconductor at zero frequency, and exists a divergence when ω tends to be infinity. The difference of $\Delta = 5/2$ from the case of $\Delta = 3/2$ is that the second pole disappears in the finite frequency as well as that the minimizing imaginary part appears. Moreover, the energy gap increasing with the parameter α implies that the larger α hinders the phase transition, which agrees with previous results. All the results with $\Delta = 5/2$ are similar to the ones in Ref. [29], especially, in Ref. [15].

3. Insulator/superconductor phase transition

Following the numerical method used above, in this section, we construct the insulator/superconductor phase transition and thus study how the Gauss–Bonnet parameter α influences the vector condensate and the conductivity. First of all, the five-dimensional Gauss–Bonnet AdS soliton reads off

$$ds^2 = -r^2 dt^2 + \frac{dr^2}{r^2 f(r)} + r^2(dx^2 + dy^2 + f(r)d\chi^2),$$
$$f(r) = \frac{1}{2\alpha}\left(1 - \sqrt{1 - \frac{4\alpha}{L^2}(1 - \frac{ML^2}{r^4})}\right), \tag{18}$$

which is obtained from the double Wick rotation to the Gauss–Bonnet AdS black hole (1), i.e., $t \to i\chi$ and $z \to it$. To distinguish the soliton from the Gauss–Bonnet AdS black hole in Sec. 2, we denote r_0 as the tip, which satisfies the condition $f(r_0) = 0$. To avoid a potential conical singularity at the tip, we impose the periodicity Γ on the spatial direction χ with $\chi \sim \chi + \pi/r_0$, i.e., $\Gamma = \pi/r_0$. As for the present soliton, there is no event horizon, thus no temperature. Moreover, because of the existence of the tip, there exists an IR cutoff for the dual field theory, which indicates a confined phase and thus similar to the mass gap in the insulator phase [9]. Therefore, it is believed that the present soliton can be used to model insulator/superconductor phase transition [19,21,38].

Now, we construct a p-wave insulator/superconductor phase transition. For the matter field, we take the form the same as the one of the conductor/superconductor phase transition, i.e., the action (4). Naturally, the form of the components for the gauge field and the matter field is taken as Eq. (7). By varying the action (4) with respect to $\psi(r)$ and $\phi(r)$, we can obtain the equations of motion

$$\psi''(r) + \left(\frac{f'(r)}{f(r)} + \frac{3}{r}\right)\psi'(r) + \left(\frac{\phi(r)^2}{r^4 f(r)} - \frac{m^2}{r^2 f(r)}\right)\psi(r) = 0, \tag{19}$$
$$\phi''(r) + \left(\frac{f'(r)}{f(r)} + \frac{3}{r}\right)\phi'(r) - \frac{2\psi(r)^2}{r^4 f(r)}\phi(r) = 0, \tag{20}$$

which are same with Eqs. (4.3) and (4.4) in Ref. [21] except the factor "2" in front of ϕ in Eq. (20) and thus expected to have the similar features about the condensate as well as the conductivity to the ones of SU(2) Yang–Mills p-wave superconductor.

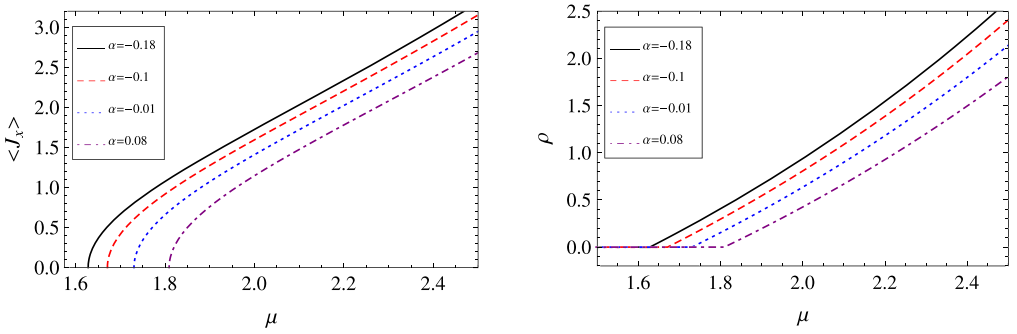

Fig. 3. The condensate (a) and charge density (b) in the case of $\Delta = 3/2$. The curves in both two subfigures from left to right correspond to $\alpha = -0.18$ (solid), -0.1 (dashed), -0.01 (dotted), 0.08 (dotdashed), respectively.

Table 2
The critical chemical potential, condensate as well as the charge density for different values of α with $\Delta = 3/2$ and $\Delta = 5/2$, where the condensate and charge density are both calculated near the critical point.

α	-0.18	-0.1	-0.01	0.08
$\mu_c(\Delta = 3/2)$	1.6280	1.6710	1.7305	1.8091
$\frac{\langle J_x\rangle}{\sqrt{\mu-\mu_c}}(\Delta_+ = 3/2)$	2.4136	2.4419	2.4435	2.4490
$\frac{\rho}{\mu-\mu_c}(\Delta = 3/2)$	2.2576	2.2292	2.1853	2.1173
$\mu_c(\Delta = 5/2)$	2.6105	2.6787	2.7730	2.8976
$\frac{\langle J_x\rangle}{\sqrt{\mu-\mu_c}}(\Delta = 5/2)$	2.5703	2.5869	2.5952	2.5629
$\frac{\rho}{\mu-\mu_c}(\Delta = 5/2)$	1.5974	1.5795	1.5490	1.4677

To numerically solve these equations, we should impose the boundary conditions at both the tip and the infinite boundary. In terms of the condition at the tip, the Neumann-like boundary condition is required to ensure $\psi(r_0)$ and $\phi(r_0)$ to be regular, while near the infinity, the general falloffs of $\psi(r)$ and $\phi(r)$ are of the form (10) and (11), respectively. Moreover, the interpretations of the coefficients ψ_-, ψ_+, μ and ρ are the same as that in the black hole from the gauge/gravity dual dictionary. By means of the symmetry of the system, $r \to \lambda r$, $\psi \to \lambda\psi$, $\phi \to \phi$, $\Gamma \to \lambda^{-1}\Gamma$, hereafter we will take $r_0 = 1$ and fix the periodicity as $\Gamma = \pi$ by rescale the vector field ψ and the gauge field ϕ. By calculations, we show the condensate and the charge density as a function of the chemical potential with $\Delta = 3/2$ in Fig. 3, from which we find that for all cases, there exists a critical chemical potential, beyond which both the vector condensate and the charge density arise. To see clearly the effect of α on the critical chemical potential and the condensate, we further list the related results in Table 2. It is observed that the critical chemical potential μ_c increases with the improving α, which means that the larger curvature correction makes the insulator/superconductor phase transition more difficult. The effect of α on the critical chemical potential is consistent with the results of Fig. 7 in Ref. [38] and similar to the one in the SU(2) p-wave model in Ref. [21]. Moreover, by fitting the curves of the condensate and the charge density, we find that they respectively behave as $\langle J_x\rangle \sim C_J\sqrt{\mu-\mu_c}$ and $\rho \sim C_\rho(\mu - \mu_c)$, which indicate that the critical exponent of the condensate as well as the charge density is respectively $1/2$ and 1, thus that the system suffers from a second-order phase transition at the critical chemical potential. To study the general behaviors, we also calculate the critical chemical potential and the condensate in the case of $\Delta = 5/2$. Due to the similarity to the case of $\Delta = 3/2$,

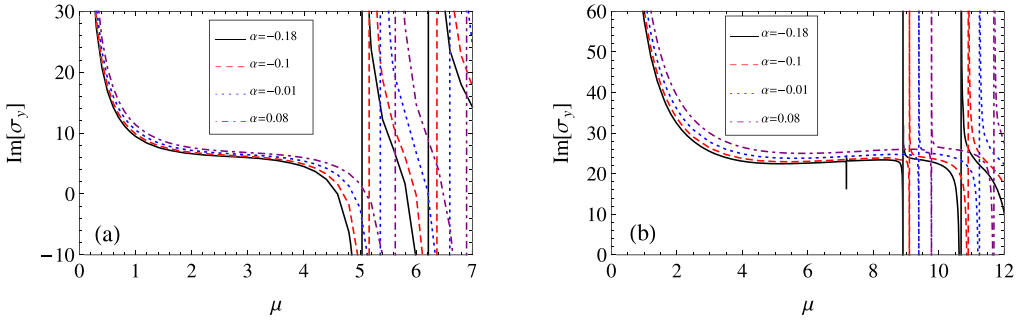

Fig. 4. The imaginary part of the AC conductivity versus the frequency in the case of $\Delta = 3/2$ with $\mu/\mu_c \approx 3$ and $\Delta = 5/2$ with $\mu/\mu_c \approx 10$. The curves in both two subfigures from left to right correspond to $\alpha = -0.18$ (solid), -0.1 (dashed), -0.01 (dotted), 0.08 (dotdashed), respectively.

we do not show the curves for the condensate and charge density for brevity but list the related results in Table 2, from which we find the behavior in the case of $\Delta = 5/2$ is indeed similar to the case of $\Delta = 3/2$, while the difference between each other is that the critical chemical potential with $\Delta = 5/2$ is larger than the one with $\Delta = 3/2$, which is reasonable, due to the fact that the dimension of the vector operator $\Delta = 5/2$ corresponds to the larger mass of the vector field.

Then, we calculate the conductivity in the five-dimensional Gauss–Bonnet AdS soliton with the vector condensate. Here, we still take the gauge perturbation perpendicular to the direction of the condensate, i.e., $\Delta A = A_y(r)e^{-i\omega t}$, with other components vanishing, from which one can read the linear equation of the perturbation as

$$A_y''(r) + \left(\frac{3}{r} + \frac{f'(r)}{f(r)}\right) A_y'(r) + \left(\frac{\omega^2}{r^4 f(r)^2} - \frac{2\psi(r)^2}{r^4 f(r)}\right) A_y(r) = 0. \tag{21}$$

To numerically solve the differential equation, we should impose the boundary conditions. Near the tip $r = r_0$, the expansion of $A_y(r)$ still includes the logarithmic term. In order to ensure the perturbation to be finite, we require the Neumann like boundary condition to eliminate the logarithmic divergence, which is similar with the condition in terms of the gauge field ϕ, thus the concrete form of $A_y(r)$ reads off

$$A_y(r) = 1 + A_{y1}(r - r_+) + A_{y2}(r - r_+)^2 + A_{y3}(r - r_+)^3 + \cdots, \tag{22}$$

while at the boundary $r \to \infty$, the expansion of $A_y(r)$ can be expressed as

$$A_x(r) = A^{(0)} + \frac{A^{(2)}}{r^2} + \frac{A^{(0)}\omega^2 L_{eff}^2}{2} \frac{log\Lambda r}{r^2} + \cdots. \tag{23}$$

Therefore, the conductivity is given by

$$\sigma(\omega) = \frac{1}{i\omega}\left(\frac{2A^{(2)}}{A^{(0)}L_{eff}^2} - \frac{\omega^2}{2}\right), \tag{24}$$

where the logarithmic divergence term in the general falloff of $A_y(r)$ is removed by the holographic renormalization.

Fig. 4 shows the imaginary part of the conductivity as a function of the frequency in the case of $\Delta = 3/2$ (a) and $\Delta = 5/2$ (b) with $\mu/\mu_c \approx 10$. Obviously, beyond the critical chemical potential, there exists a pole (corresponding to a delta function in the real part) at the zero frequency,

which is expected from the standpoint of the superconductor. Moreover, when the parameter α increases, the location of the second pole of the imaginary part increases, which means that the energy of the quasiparticle excitation increases with the improving Gauss–Bonnet gravitational correction. In addition, the conductivity with $\Delta = 5/2$ is similar with the case of $\Delta = 5/2$.

4. Conclusions and discussions

So far, we have numerically constructed the p-wave superconductors in the Gauss–Bonnet gravity at the level of the probe approximation. Concretely, we mainly studied the effects of the high curvature correction on the conductor/superconductor and insulator/superconductor phase transition, respectively, and further observed the transport phenomenon for the superconductor. The main conclusions can be summarized as follows.

In terms of the p-wave conductor/superconductor phase transition in the five-dimensional Gauss–Bonnet AdS black hole, the critical temperature increases with the parameter α, which indicates that the larger Gauss–Bonnet curvature correction hinders the phase transition. Moreover, the improving dimension of the vector operator Δ also makes the transition more difficult, because the larger Δ corresponds to the larger "mass" in the dual field theory. What is more, at the critical point, the critical exponent of the vector condensate is $1/2$, which means that the system suffers from a second-order transition as expected from the mean field theory. When the temperature decreases gradually from the critical value, the vector condensate tends to be a stable value increasing with the Gauss–Bonnet parameter α. In addition, in the background of black hole with the vector 'hair', we observed the delta function at zero frequency, which is the signal of the infinite DC conductivity and agrees with the superconductivity. Besides, we find the ratio of the energy gap and the critical temperature increases with the larger α, which is consistent with the fact the larger α decreases the critical temperature. Meanwhile, for all case of the parameter α, the ratio of the energy gap and the critical temperature is much larger than the BCS value 3.5, which implies that the holographic model indeed includes the strong interaction.

As for the insulator/superconductor phase transition, the critical chemical potential increases with the larger α, which suggests that the larger α inhibits the superconductor phase transition. Moreover, the critical chemical potential with $\Delta = 5/2$ is larger than the one with $\Delta = 3/2$ when the Gauss–Bonnet parameter α is fixed. Furthermore, near the critical point, the critical exponent of the vector condensate and the charge density is $1/2$ and 1, respectively, which means that the system undergoes a second-order phase transition. In addition, when the parameter α increases, the location of the second pole of the imaginary part moves toward right, which indicates that the energy of the quasiparticle excitation increases with α.

In a word, the increasing Gauss–Bonnet correction α (the dimension of the vector operator Δ) always inhibits both the conductor/superconductor and insulator/superconductor transition. Near the critical point, both systems undergo a second-order phase transition. The stable value of the vector condensate increases with the larger α in the Gauss–Bonnet AdS black hole. The ratio of the energy gap and the critical value much larger than the BCS value indicates the holographic models indeed simulate the strong interaction. The features of MCV superconductor model are similar to the ones of the SU(2) p-wave model in both black hole and soliton backgrounds. Therefore, our results shed light on understanding the strong interacting system from the perspective of the gravity/gauge duality to some extent. It should be noted that we have only numerically constructed the superconductor model and not studied the critical value as well as the critical behaviors of the vector condensate, but the analytical results in Ref. [38] can back up our numerical results to some extent. Of course, to systematically study the effects of α on the MCV model, it is

helpful to calculate the critical value by the Sturm–Liouville method [6] as well as the Matching method [14]. For simplicity, we did not calculate the transport along the condensing direction, which is certainly different from the feature of $A_y(r)$ and will provide more interesting physics for us, therefore, it is useful to systematically calculate the perturbation along the condensate, and further explore the transport phenomenon for the superconductor. Meanwhile, it is worth stressing that we study the MCV model at the probe approximation. We have not observed the rich phase structure appeared in Refs. [18,39–41,45]. To further understand the influence of high curvature correction on the holographic superconductor phase transition, in the near future, we will study the backreaction of this MCV model in the Gauss–Bonnet–AdS gravity and then find the boundaries of the phase diagram in the parameter spacetime.

Acknowledgements

We would like to thank Prof. R.G. Cai and Dr. L. Li for their helpful discussions and comments. This work is supported in part by the National Natural Science Foundation of China (Nos. 11475143, 11175077 and 11575075), HASTIT (No. 14HASTIT043), the Joint Specialized Research Fund for the Doctoral Program of Higher Education, Ministry of Education of Peoples's Republic of China (No. 20122136110002), the Joint Fund Project of Science and Technology Department in Guizhou Province (No. Qian Ke He LH Zi[2015]7709) and the Foundation of Scientific Innovative Research Team of Education Department of Guizhou Province (201329).

References

[1] J.M. Maldacena, The large N limit of superconformal field theories and supergravity, Adv. Theor. Math. Phys. 2 (1998) 231, arXiv:hep-th/9711200.
[2] S.S. Gubser, I.R. Klebanov, A.M. Polyakov, Gauge theory correlators from noncritical string theory, Phys. Lett. B 428 (1998) 105, arXiv:hep-th/9802109.
[3] S.A. Hartnoll, C.P. Herzog, G.T. Horowitz, Building a holographic superconductor, Phys. Rev. Lett. 101 (2008) 031601, arXiv:0803.3295 [hep-th].
[4] S.S. Gubser, S.S. Pufu, The gravity dual of a p-wave superconductor, J. High Energy Phys. 0811 (2008) 033, arXiv:0805.2960 [hep-th].
[5] J.W. Chen, Y.J. Kao, D. Maity, W.Y. Wen, C.P. Yeh, Towards a holographic model of D-wave superconductors, Phys. Rev. D 81 (2010) 106008, arXiv:1003.2991 [hep-th].
[6] G. Siopsis, J. Therrien, Analytic calculation of properties of holographic superconductors, J. High Energy Phys. 1005 (2010) 013, arXiv:1003.4275 [hep-th].
[7] S. Kanno, A note on Gauss–Bonnet holographic superconductors, Class. Quantum Gravity 28 (2011) 127001, arXiv:1103.5022 [hep-th].
[8] S.A. Hartnoll, C.P. Herzog, G.T. Horowitz, Holographic superconductors, J. High Energy Phys. 0812 (2008) 015, arXiv:0810.1563 [hep-th].
[9] T. Nishioka, S. Ryu, T. Takayanagi, Holographic superconductor/insulator transition at zero temperature, J. High Energy Phys. 1003 (2010) 131, arXiv:0911.0962 [hep-th].
[10] T. Albash, C.V. Johnson, A holographic superconductor in an external magnetic field, J. High Energy Phys. 0809 (2008) 121, arXiv:0804.3466 [hep-th].
[11] E. Nakano, W.Y. Wen, Critical magnetic field in a holographic superconductor, Phys. Rev. D 78 (2008) 046004, arXiv:0804.3180 [hep-th].
[12] R.G. Cai, Gauss–Bonnet black holes in AdS spaces, Phys. Rev. D 65 (2002) 084014, arXiv:hep-th/0109133.
[13] R.G. Cai, S.P. Kim, B. Wang, Ricci flat black holes and Hawking–Page phase transition in Gauss–Bonnet gravity and dilaton gravity, Phys. Rev. D 76 (2007) 024011, arXiv:0705.2469 [hep-th].
[14] R. Gregory, S. Kanno, J. Soda, Holographic superconductors with higher curvature corrections, J. High Energy Phys. 0910 (2009) 010, arXiv:0907.3203 [hep-th].
[15] R.G. Cai, Z.Y. Nie, H.Q. Zhang, Holographic p-wave superconductors from Gauss–Bonnet gravity, Phys. Rev. D 82 (2010) 066007, arXiv:1007.3321 [hep-th].

[16] Q. Pan, B. Wang, General holographic superconductor models with Gauss–Bonnet corrections, Phys. Lett. B 693 (2010) 159, arXiv:1005.4743 [hep-th].
[17] H.F. Li, R.G. Cai, H.Q. Zhang, Analytical studies on holographic superconductors in Gauss–Bonnet gravity, J. High Energy Phys. 1104 (2011) 028, arXiv:1103.2833 [hep-th].
[18] R.G. Cai, Z.Y. Nie, H.Q. Zhang, Holographic phase transitions of P-wave superconductors in Gauss–Bonnet gravity with back-reaction, Phys. Rev. D 83 (2011) 066013, arXiv:1012.5559 [hep-th].
[19] Q. Pan, B. Wang, E. Papantonopoulos, J. Oliveira, A.B. Pavan, Holographic superconductors with various condensates in Einstein–Gauss–Bonnet gravity, Phys. Rev. D 81 (2010) 106007, arXiv:0912.2475 [hep-th].
[20] S. Gangopadhyay, D. Roychowdhury, Analytic study of Gauss–Bonnet holographic superconductors in Born–Infeld electrodynamics, J. High Energy Phys. 1205 (2012) 156, arXiv:1204.0673 [hep-th].
[21] Q. Pan, J. Jing, B. Wang, Analytical investigation of the phase transition between holographic insulator and superconductor in Gauss–Bonnet gravity, J. High Energy Phys. 1111 (2011) 088, arXiv:1105.6153 [gr-qc].
[22] S.l. Cui, Z. Xue, Critical magnetic field in a holographic superconductor in Gauss–Bonnet gravity with Born–Infeld electrodynamics, Phys. Rev. D 88 (10) (2013) 107501, arXiv:1306.2013 [hep-th].
[23] W. Yao, J. Jing, Analytical study on holographic superconductors for Born–Infeld electrodynamics in Gauss–Bonnet gravity with backreactions, J. High Energy Phys. 1305 (2013) 101, arXiv:1306.0064 [gr-qc].
[24] X.Y. Guo, L.C. Zhang, R. Zhao, An analytic analysis of d-dimensional Gauss–Bonnet holographic superconductor in Born–Infeld electrodynamics, Mod. Phys. Lett. A 29 (19) (2014) 1450083.
[25] O. Miskovic, L. Aranguiz, Gauss–Bonnet holographic superconductors, The Thirteenth Marcel Grossmann Meeting: pp. 1425–1427, http://dx.doi.org/10.1142/9789814623995_0192.
[26] Z.Y. Nie, H. Zeng, P–T phase diagram of a holographic s + p model from Gauss–Bonnet gravity, J. High Energy Phys. 1510 (2015) 047, arXiv:1505.02289 [hep-th].
[27] D. Ghorai, S. Gangopadhyay, Analytic study of higher dimensional holographic superconductors in Born–Infeld electrodynamics away from the probe limit, arXiv:1511.02444 [hep-th].
[28] G. Liu, Y. Peng, A general Stückelberg holographic conductor/superconductor model, Mod. Phys. Lett. A 30 (2015) 1550183.
[29] G.T. Horowitz, M.M. Roberts, Holographic superconductors with various condensates, Phys. Rev. D 78 (2008) 126008, arXiv:0810.1077 [hep-th].
[30] G.T. Horowitz, Introduction to holographic superconductors, Lect. Notes Phys. 828 (2011) 313, arXiv:1002.1722 [hep-th].
[31] G.T. Horowitz, M.M. Roberts, Zero temperature limit of holographic superconductors, J. High Energy Phys. 0911 (2009) 015, arXiv:0908.3677 [hep-th].
[32] R.G. Cai, S. He, L. Li, L.F. Li, A holographic study on vector condensate induced by a magnetic field, J. High Energy Phys. 1312 (2013) 036, arXiv:1309.2098 [hep-th].
[33] K. Wong, A non-abelian vortex lattice in strongly coupled systems, J. High Energy Phys. 1310 (2013) 148, arXiv:1307.7839 [hep-th].
[34] M.N. Chernodub, Spontaneous electromagnetic superconductivity of vacuum in strong magnetic field: evidence from the Nambu–Jona–Lasinio model, Phys. Rev. Lett. 106 (2011) 142003, arXiv:1101.0117 [hep-ph].
[35] F. Levy, I. Sheikin, B. Grenier, A. Huxley, Magnetic field-induced superconductivity in the ferromagnet URhGe, Science 309 (2005) 1343.
[36] R.G. Cai, L. Li, L.F. Li, Y. Wu, Vector condensate and AdS soliton instability induced by a magnetic field, J. High Energy Phys. 1401 (2014) 045, arXiv:1311.7578 [hep-th].
[37] Y.B. Wu, J.W. Lu, M.L. Liu, J.B. Lu, C.Y. Zhang, Z.Q. Yang, Lifshitz effects on vector condensate induced by a magnetic field, Phys. Rev. D 89 (10) (2014) 106006, arXiv:1403.5649 [hep-th].
[38] Y.B. Wu, J.W. Lu, Y.Y. Jin, J.B. Lu, X. Zhang, S.Y. Wu, C. Wang, Magnetic-field effects on p-wave phase transition in Gauss–Bonnet gravity, Int. J. Mod. Phys. A 29 (2014) 1450094, arXiv:1405.2499 [hep-th].
[39] R.G. Cai, L. Li, L.F. Li, A holographic P-wave superconductor model, J. High Energy Phys. 1401 (2014) 032, arXiv:1309.4877 [hep-th].
[40] L.F. Li, R.G. Cai, L. Li, C. Shen, Entanglement entropy in a holographic p-wave superconductor model, Nucl. Phys. B 894 (2015) 15, arXiv:1310.6239 [hep-th].
[41] R.G. Cai, L. Li, L.F. Li, R.Q. Yang, Towards complete phase diagrams of a holographic P-wave superconductor model, J. High Energy Phys. 1404 (2014) 016, arXiv:1401.3974 [gr-qc].
[42] R.G. Cai, L. Li, L.F. Li, R.Q. Yang, Introduction to holographic superconductor models, Sci. China, Phys. Mech. Astron. 58 (6) (2015) 060401, arXiv:1502.00437 [hep-th].
[43] E. Kiritsis, L. Li, Holographic competition of phases and superconductivity, arXiv:1510.00020 [cond-mat.str-el].
[44] R.G. Cai, R.Q. Yang, Coexistence and competition of ferromagnetism and p-wave superconductivity in holographic model, Phys. Rev. D 91 (2) (2015) 026001, arXiv:1410.5080 [hep-th].

[45] P. Chaturvedi, G. Sengupta, p-Wave holographic superconductors from Born–Infeld black holes, J. High Energy Phys. 1504 (2015) 001, arXiv:1501.06998 [hep-th].
[46] L. Zhang, Q. Pan, J. Jing, Holographic p-wave superconductor models with Weyl corrections, Phys. Lett. B 743 (2015) 104, arXiv:1502.05635 [hep-th].
[47] M. Rogatko, K.I. Wysokinski, P-wave holographic superconductor/insulator phase transitions affected by dark matter sector, arXiv:1508.02869 [hep-th].
[48] Y.B. Wu, J.W. Lu, W.X. Zhang, C.Y. Zhang, J.B. Lu, F. Yu, Holographic p-wave superfluid, Phys. Rev. D 90 (12) (2014) 126006, arXiv:1410.5243 [hep-th].
[49] Y.B. Wu, J.W. Lu, C.Y. Zhang, N. Zhang, X. Zhang, Z.Q. Yang, S.Y. Wu, Lifshitz effects on holographic p-wave superfluid, Phys. Lett. B 741 (2014) 138, arXiv:1412.3689 [hep-th].
[50] A. Buchel, R.C. Myers, Causality of holographic hydrodynamics, J. High Energy Phys. 0908 (2009) 016, arXiv:0906.2922 [hep-th].
[51] R.G. Cai, H.Q. Zhang, Holographic superconductors with Horava–Lifshitz black holes, Phys. Rev. D 81 (2010) 066003, arXiv:0911.4867 [hep-th].
[52] J.W. Lu, Y.B. Wu, P. Qian, Y.Y. Zhao, X. Zhang, Lifshitz scaling effects on holographic superconductors, Nucl. Phys. B 887 (2014) 112, arXiv:1311.2699 [hep-th].